

2004

Ferromagnetism in Cr-doped GaN: A first-principles calculation

G. P. Das

Virginia Commonwealth University, Bhabha Atomic Research Centre

B. K. Rao

Virginia Commonwealth University

Puru Jena

Virginia Commonwealth University, pjena@vcu.edu

Follow this and additional works at: http://scholarscompass.vcu.edu/phys_pubs

 Part of the [Physics Commons](#)

Das, G.P., Rao, B.K., Jena, P. Ferromagnetism in Cr-doped GaN: A first-principles calculation. *Physical Review B*, 69, 214422 (2004). Copyright © 2004 American Physical Society.

Downloaded from

http://scholarscompass.vcu.edu/phys_pubs/99

This Article is brought to you for free and open access by the Dept. of Physics at VCU Scholars Compass. It has been accepted for inclusion in Physics Publications by an authorized administrator of VCU Scholars Compass. For more information, please contact libcompass@vcu.edu.

Ferromagnetism in Cr-doped GaN: A first-principles calculationG. P. Das,^{1,2} B. K. Rao,¹ and P. Jena¹¹*Department of Physics, Virginia Commonwealth University, Richmond, Virginia 23284-2000, USA*²*Bhabha Atomic Research Centre, TPEP, Physics Group, Mumbai 400 085, India*

(Received 3 April 2003; revised manuscript received 11 July 2003; published 24 June 2004)

Electronic structure, energy bands, and magnetic properties of Cr-doped GaN have been calculated from first principles using a 32 atom supercell within the frame work of linearized muffin-tin orbital tight binding method and gradient-corrected density-functional theory. The coupling between Cr atoms is found to be ferromagnetic with a magnetic moment of $2.69\mu_B$ at each Cr site. The magnetic moments of Ga and N sites are rather small, namely, $0.025\mu_B$ and $-0.025\mu_B$, respectively, yielding a total moment of $6\mu_B$ per supercell. Parallel calculations done on small clusters of Cr-doped GaN also yield similar results indicating that magnetic coupling between Cr atoms results from a local phenomenon. These results are consistent with the recent experimental discovery of ferromagnetism in Cr-doped GaN single crystals.

DOI: 10.1103/PhysRevB.69.214422

PACS number(s): 75.30.Hx, 72.80.Ey, 75.50.Pp

I. INTRODUCTION

The interplay between the charge carriers in a semiconductor and the electron spins of a ferromagnetic metal doped into the semiconductor can be utilized for many magneto/spin-electronic devices. The desirable features for the successful application of a semiconductor spintronics material are that it should show ferromagnetism with a reasonably high T_C , and a sizable concentration of magnetic sites. There should also be some efficient mechanism to inject spin-polarized charge carriers from a metal into or across a non-magnetic semiconductor. Interest in the family of carrier-induced dilute magnetic semiconductors (DMS) started with the discovery of ferromagnetism in $\sim 5\%$ Mn-doped InAs and GaAs with a Curie point of 110 K ¹ and the subsequent theoretical prediction^{2,3} that the Curie point in Mn-doped GaN could be higher than the room temperature. Amongst the III-V semiconductors, GaN, with a wide-band gap of $\sim 3.4\text{ eV}$, is extensively studied because of its promising applications in short wavelength opto-electronic devices.⁴ Although wurtzite-structured ferromagnetic $\text{Mn}_x\text{Ga}_{1-x}\text{N}$ samples have been grown using various techniques, there is a wide variation in the reported magnitude of Curie temperature (T_C) in Mn:GaN.

The recent discovery⁵ of the room temperature ferromagnetism of Cr-doped GaN single crystals has stirred further interest in the DMS systems. This discovery is significant because Cr-doped GaN has been successfully grown in the form of bulk single crystals using a sodium flux growth method. In contrast, Mn-doped GaN samples are grown in the form of thin films.⁶ The ferromagnetic to paramagnetic transition temperature (T_C) of (Ga,Cr)N is observed to be around 280 K from superconducting quantum interference device (SQUID) magnetization measurement as well as from the temperature dependence of electrical resistivity that shows a change in slope at $\sim 280\text{ K}$. A higher T_C ($\geq 400\text{ K}$) has also been reported for the thin films of (Ga,Cr)N grown on a sapphire substrate by the electron cyclotron resonance assisted molecular-beam-epitaxy (ECR-MBE) technique.⁷ However, in the case of thin films, the

contribution of substrates plays a crucial role. The x-ray diffraction pattern of bulk (Ga,Cr)N single crystals clearly shows a wurtzite structure with $c=5.191\text{ \AA}$, which is marginally larger than that of pure GaN ($c=5.185\text{ \AA}$). This is attributed to the larger Cr atomic radius (1.40 \AA) than Ga (1.26 \AA), indicating that Cr indeed substitutes the Ga site. When doped into GaN and Cr, Mn atoms go to the Ga-substitutional site as Cr^{3+} and Mn^{3+} valence states in d^3 and d^4 configurations, respectively. This indicates that a magnetic impurity such as Mn or Cr contributes spins as well as holes (p -type doping) to the III-V semiconductors such as GaN.

The first attempt to explain carrier-controlled ferromagnetism in Mn-doped III-V semiconductors was made by Dietl *et al.*² who used the double-exchange Zener model⁸ of ferromagnetism and predicted how the incorporation of Mn ions induces ferromagnetic behavior via hole-mediated exchange interaction (Ruderman-Kittel-Kasuya-Yosida type). Litvinov and Dugaev⁹ subsequently proposed the indirect exchange interaction caused by virtual electron excitations from magnetic impurity acceptor levels to the valence band. *Ab initio* calculations¹⁰⁻¹³ have also been carried out to understand the underlying mechanism of carrier-induced ferromagnetism in transition-metal (TM) -doped III-V and II-VI semiconductors. Basically there are two approaches, both based on density-functional theory, viz., (a) the supercell approach in which the TM impurity atom is placed in the substitutional Ga site in a large supercell (size depending on the impurity concentration) such that the impurities in two neighboring cells do not interact; (b) the coherent potential approximation (CPA) approach, which treats the DMS as a randomly disordered substitutional alloy. Schilfgaarde and Mryasov¹⁰ have performed a thorough investigation of the anomalous magnetic interactions in doped DMS systems. They had performed linearized muffin-tin orbital (LMTO) calculations on a zinc-blende structured supercell, in order to investigate the exchange interactions between $3d$ magnetic dopants (Cr, Mn, and Fe) in different III-V semiconductors (GaAs, GaN, and AlN). They had observed that doping caused deviations in the magnetic exchange interaction from what is predicted by simple models due to the formation of

deep levels. They also concluded that short-range interaction between the dopant atoms could cause a clustering of these atoms. More recently, Kronik *et al.*¹¹ performed plane wave pseudopotential-based supercell calculations, in order to examine the theoretical limits to spin-polarized transport in wurtzite $\text{Mn}_x\text{Ga}_{1-x}\text{N}$ for 6% Mn doping. From their band structure calculations they inferred that $\text{Mn}_x\text{Ga}_{1-x}\text{N}$ is more suitable for spin injection, compared to $\text{Mn}_x\text{Ga}_{1-x}\text{As}$. Sato and Katayama-Yoshida¹² used the Korringa-Kohn-Rostoker coherent potential approximation (KKR-CPA) on various $3d$ TM-doped disordered DMS systems (both III-V and II-VI). They found the ferromagnetic state to be stable for less than (or equal to) half-filled V, Cr, and Mn doping, while a spin-glass-like state is stable for more than half-filled Fe, Co, and Ni doping. Similar conclusions have also been arrived at by Schilfgaard and Mryasov,¹⁰ who have provided explanations for this in terms of the Anderson-Hasegawa model. This inference is reiterated by the experimental observations of ferromagnetism in Mn- and Cr-doped GaN. Recently Rao and Jena¹³ have shown that the bond strength of Mn-N is significantly larger than that of Ga-N bond strength. This implies that substitution of Mn at the Ga site is energetically favorable. In addition, it may also lead to a clustering of Mn around the N site. They found the Mn atoms to be coupled ferromagnetically, leading to giant magnetic moments. Schilfgaard and Mryasov¹⁰ have also arrived at similar conclusions for the clustering of the magnetic impurities.

In this work, we have carried out a first-principles investigation of the (Ga,Cr)N system using two different techniques. Using a super-cell technique, we have replaced two nearest neighbor Ga sites with Cr atoms in wurtzite GaN crystal and calculated the magnetic structure using spin-polarized density-functional theory. We have also carried out parallel calculations in Cr-doped GaN clusters. Since GaN clusters have different structures than their bulk, the objective of the cluster studies was to see if the Cr-Cr magnetic coupling depends on its environment and on Cr-Cr interatomic distance. Our *ab initio* investigations yield the electronic structure, energetics, and magnetism of Cr-doped GaN in a cluster as well as in a bulk crystalline environment. In Sec. II we outline our computational procedure. The results are discussed in Sec. III and summarized in Sec. IV.

II. COMPUTATIONAL DETAILS

In order to simulate the effect of doping a Cr_2 dimer in Ga substitutional sites, and to see if there is ferromagnetic coupling between Cr spins governed by its local environment, we have performed two sets of calculations: (a) supercell band structure calculations with the cation (Ga) site selectively replaced by Cr atoms and (b) *ab initio* cluster calculation with a Cr_2 dimer embedded inside a $(\text{GaN})_x$ cluster. All the results reported in this work are based on the density-functional theory with the gradient-corrected exchange-correlation functional.¹⁴

A. Supercell band calculations

For our supercell calculations, we have used the experimental lattice parameters obtained in the recent work on bulk

(Ga,Cr)N single crystals whose x-ray diffraction pattern clearly shows a wurtzite structure with $a=3.18 \text{ \AA}$ and $c=5.191 \text{ \AA}$. The c/a ratio of 1.628, which is slightly larger than that of pure GaN, is due to the larger Cr atomic radius (1.40 \AA) compared to that of Ga (1.26 \AA). The corresponding Ga-N bond length is 1.947 \AA . In the wurtzite structure, the lattice vectors are (in units of a) $(\sqrt{3}/2, -1/2, 0)$, $(0, 1, 0)$ and $(0, 0, c/a)$. The unit cell contains two cations at $(0,0,0)$ and $(2/3, 1/3, 1/2)$, and two anions at $(0,0,3/8)$ and $(2/3, 1/3, 7/8)$. We have constructed a 32 atom supercell composed of eight wurtzite primitive cells of GaN, i.e., the lattice vectors have been doubled along all three directions, thereby accommodating 16 Ga and 16 N atoms. For studying Cr-doped GaN, we replaced a pair of neighboring Ga atoms by Cr atoms so that the supercell formula unit becomes $\text{Cr}_2\text{Ga}_{14}\text{N}_{16}$. The reason for substituting two Ga atoms by Cr is to allow the Cr spins the freedom to couple ferromagnetically or antiferromagnetically. We should point out that the 32 atom supercell is one of the smallest supercells that ensures separation between the impurities in neighboring supercells by at least a few times the Ga-N bond length. The Cr-Cr separation can be varied within the supercell in the range of $\sim 3-5 \text{ \AA}$. The results reported here have been performed with Cr-Cr distance of 3.2 \AA , which is more than the critical separation of $\sim 2.7 \text{ \AA}$ needed for ferromagnetic coupling to occur. This value has been obtained from our cluster calculation, which will be discussed in Sec. III B.

We have used the self-consistent tight-binding linear muffin-tin orbital (TB-LMTO) method¹⁵ with the atomic sphere approximation (ASA) and incorporated the ‘‘combined correction’’ term that accounts for the non-ASA contribution to the overlap matrix. Knowing the ASA potential, one can calculate the ground-state charge density, and hence the ASA total energy. We have used the gradient-corrected spin-polarized exchange-correlation functional as per the original Perdew-Wang formulation.¹⁴ All of our calculations have been performed scalar relativistically, i.e., without spin-orbit interaction, which is not significant in the case of GaN. Spin-polarized bands have been calculated with a minimal basis set consisting of s , p , and d orbitals ($\ell=2$) for Ga, Cr, and N, with N- d orbitals downfolded. The need for treating the localized semicore $3d$ states of Ga as band states has already been emphasized by other workers,^{16,17} and accordingly we have included the fully occupied $3d$ states of Ga as relaxed band states in our self-consistent iterations. Apart from the valence states of Ga, Cr, and N, the core orbitals were kept frozen in their isolated atomic form. In order to fix the magnitudes of the sphere radii of the individual atoms, we have used the so-called Hartree potential plot prescription.¹⁸ This yields Ga and N atomic sphere radii to be 1.227 and 1.015 \AA , which are roughly proportional to the corresponding covalent radii of 1.62 and 1.26 \AA of Ga and N, respectively. And for Cr, we have used the same atomic sphere radius as that of Ga. Since the wurtzite GaN is an open structure, which is typical of any tetrahedrally bonded semiconductor, we have introduced two different types of empty spheres (two of each type) at the high symmetry positions consistent with the $P6_3mc$ space group. Thus the wurtzite unit cell is divided into a total of eight overlapping

atomic spheres (four real atoms and four empty spheres). This translates to a 64 sphere supercell, i.e., 32 real atoms and 32 empty spheres. In all our supercell calculations, we have used (6,6,4) \mathbf{k} mesh, which corresponds to 144 \mathbf{k} points in the irreducible wedge of the simple cubic Brillouin Zone (BZ). BZ integration has been performed using the improved tetrahedron method¹⁹ that avoids misweighing and corrects errors due to the linear approximation of the bands inside each tetrahedron. In order to establish the location and occupancy of the impurity band in the gap, we have calculated the so-called “fat bands” which are nothing but the band structure projected onto specific site orbitals. The projected impurity bands are fattened, and the widths allocated are proportional to the sum of the weights of the corresponding orthonormal orbitals.¹⁸

B. Cluster calculations

We have studied atomic clusters of $\text{Cr}_2(\text{GaN})_x$ ($x \leq 3$). In this size range, almost all the Ga and N atoms are surface atoms, and consequently, have dangling bonds. Interaction of the Cr atoms with the Ga and N atoms not only can alter the structure of $(\text{GaN})_x$ clusters, but also can influence their magnetic coupling with each other. We should emphasize that the nearest neighbor configuration of Cr atoms, the Cr-Cr interatomic distance, and the coordination of Ga and N atoms in $\text{Cr}_2(\text{GaN})_x$ clusters are expected to be very different from those in the bulk. Thus, the magnetic properties of $\text{Cr}_2(\text{GaN})_x$ clusters will provide a good test of how sensitive the Cr-Cr magnetic coupling is to its environment, and may illustrate the importance of lattice relaxation on the magnetic coupling between Cr atoms in GaN crystal. We have studied this problem by using the linear combination of the atomic orbitals-molecular orbital (LCAO-MO) method and the gradient-corrected density-functional theory. The equilibrium geometries of $(\text{GaN})_x$ and $\text{Cr}_2(\text{GaN})_x$ clusters are computed by optimizing their structures with respect to different arrangements as well as spin configurations. Since the clusters have a finite number of electrons occupying discrete molecular energy levels, their preferred spin multiplicity ($M=2S+1$) yields the number of unpaired electrons and hence the total magnetic moment. An analysis of the spin density distribution and the Mulliken population yields the directions of the spin moments (up or down) and hence, the magnetic coupling. We have used frozen core LANL2DZ basis sets for the atomic orbitals and the calculations were performed using the Gaussian 98 code.²⁰ We have used the Becke, Perdew, Wang²¹ (commonly referred to as BPW91) prescription for the generalized gradient approximation (GGA) form of the exchange correlation potentials. The threshold of the root mean square forces for geometry optimization was set at 0.0003 a.u./Bohr. Calculations were carried out for various spin multiplicities of each cluster. The lowest energy configuration then yields the total magnetic moment, $(M-1)\mu_B$ of the cluster. For Cr_2 in GaN, we have found that the total energy for ferromagnetic coupling is lower in energy by 0.42 eV compared to the antiferromagnetic configuration. Accordingly, the results reported in the following section are all based on ferromagnetic configuration only.

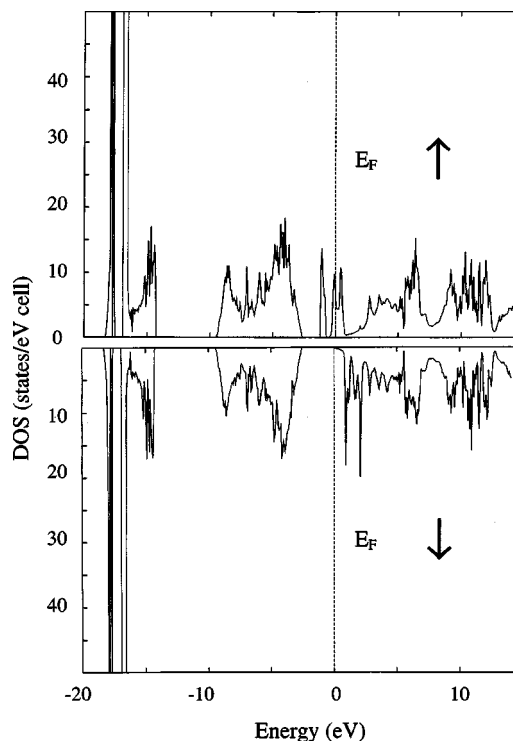


FIG. 1. Total density of states of $(\text{Ga}_{14}\text{Cr}_2)\text{N}_{16}$ supercell for majority spin (top) and minority spin (bottom).

III. RESULTS AND DISCUSSION

A. Cr_2 -doped GaN crystal

Many of the salient features of the electronic structure of the $(\text{Ga,Cr})\text{N}$ system can be seen from the total spin density of states (DOS) per unit supercell (Fig. 1) and the partial DOS of the Cr impurity atom (Fig. 2). First of all, we observe a half-metallic behavior in the sense that the Fermi level state density is finite for the majority spin and zero for the minority spin. This half-metallicity is due to Cr-3d hybridizing with the N-2p states. The Cr d band with a three-peaked structure and a width of ~ 2 eV falls within the LDA gap of GaN, which is lower than the experimental gap as expected. There is still controversy in the literature as to whether such DMS systems are strictly half-metallic or whether the semiconducting nature of the material is retained upon doping.¹¹ Both the doubly degenerate e_g bands and the triply degenerate t_{2g} bands, of Cr are strongly spin split by ~ 1.8 eV. While the majority states of Cr lie within the GaN band gap, as can be seen from the ℓ -projected fat bands²² (Fig. 3), the minority states merge with the conduction band states. The Cr- e_g and Cr- t_{2g} projected fat bands crossing the Fermi level point towards d^3 configuration of Cr in GaN, as compared to a d^4 configuration of Mn in GaN that we have found in a similar analysis performed earlier.²³ This is also similar to what was found by Schilfgaard and Mryasov¹⁰ in their study of doped DMS systems. The bonding peak for the Cr majority spin lies ~ 1.5 eV above the valence band top, which matches with the estimate given by van Schilfgaard and Mryasov.¹⁰ This implies that Cr acts as an acceptor just like Mn. It is to be noted that here the 3d states lay around

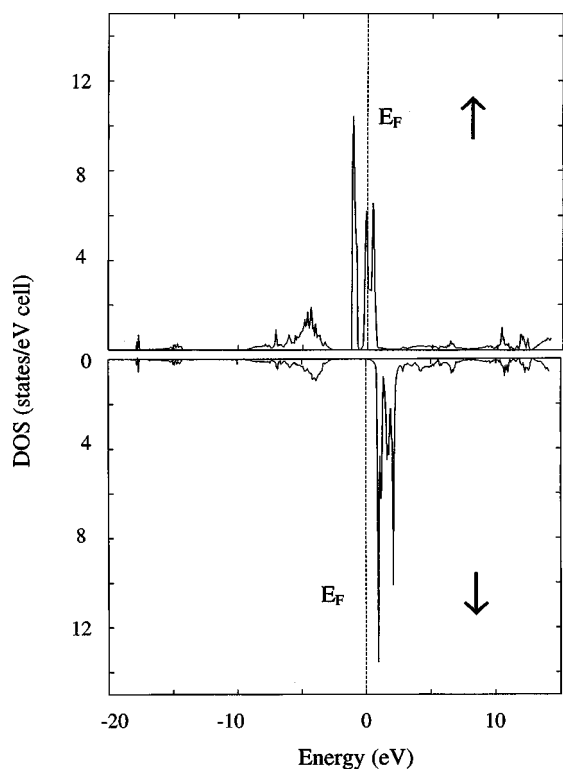


FIG. 2. Partial DOS of Cr in $(\text{Ga}_{14}\text{Cr}_2)\text{N}_{16}$ supercell majority spin (top) and minority spin (bottom).

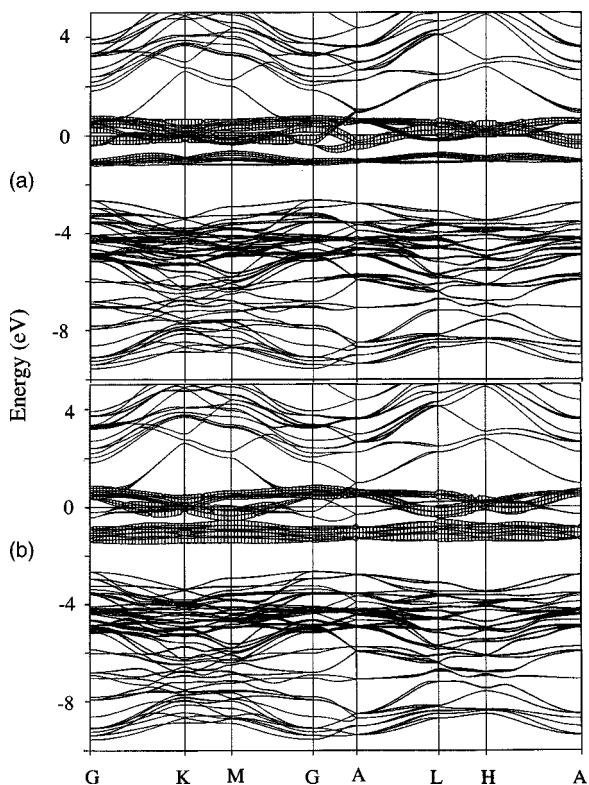


FIG. 3. Cr-projected fat bands for majority spin (a) e_g projected (b) t_{2g} projected.

the midgap, in contrast with the case of $(\text{GaMn})\text{As}$, where the d bands of manganese lay just above the valence band edge.¹⁰

We have also studied the paramagnetic DOS (i.e., before switching on the spin polarization) to check the exact position of the e_g and the t_{2g} bands of Cr in the $(\text{Ga,Cr})\text{N}$ supercell DOS. The fact that the t_{2g} levels lie above e_g confirms that Cr is sitting in the tetrahedral environment in the GaN lattice. Had it been the other way (i.e., e_g above t_{2g}) then the crystal-field splitting would have suggested Cr in octahedral environment. This is in tune with what Sato *et al.*¹² and Schilfgaard and Myrasov¹⁰ have mentioned in their papers. Subsequently, when spin polarization is switched on, the ferromagnetic calculation shows a further spin splitting which we observe in our partial DOS as well as in fat bands.

Our calculations show that $\text{Cr}_2\text{Ga}_{14}\text{N}_{16}$ is having a ferromagnetic ground state with a localized magnetic moment of $2.69\mu_B$ on the Cr atoms. The nearest neighbor host atoms are weakly polarized (induced moments of $+0.025\mu_B$ on nearest neighbor Ga sites and $-0.025\mu_B$ on nearest neighbor N sites). Note that this nonintegral value of the magnetic moment is due to the use of the atomic sphere approximation in our self-consistent calculation. Similar calculations that we had performed earlier²³ on the $\text{Mn}_2\text{Ga}_{14}\text{N}_{16}$ supercell had shown a magnetic moment of $3.5\mu_B$ on the Mn atom. Thus, doping of GaN by Mn or Cr, both of which are nearly half-filled bands leads to ferromagnetism. This result agrees with the conclusion derived from KKR-CPA calculations,¹² and LMTO calculations¹⁰ where the authors reported the trend in the magnetic states when different $3d$ transition metals are doped into III-V as well as II-VI semiconductors. They also had arrived at the conclusion that Cr- and Mn-doped GaN DMS's are both ferromagnetic. It is to be noted that the increase of Cr-Cr separation in the supercell, or the incorporation of Cr in the interstitial site leads to drastic reduction in the magnetic coupling.

B. Cr-doped $(\text{GaN})_x$ clusters

In order to demonstrate the sensitivity of the magnetic coupling between two Cr atoms to its interatomic distance and environment, we have studied an extreme case, namely Cr atoms doped into $(\text{GaN})_x$ clusters. As already mentioned, Schilfgaard and Myrasov¹⁰ have also studied the effect of the dependence of the environment on the magnetic interaction in the case of doped DMS systems. From time to time we shall compare our results with some of their results as relevant. We note that the structure and coordination in atomic clusters are very different from their bulk. Thus, a Cr_2 dimer doped into $(\text{GaN})_x$ clusters may have different interatomic separation and environments, and this could change significantly with the size, x . We have performed self-consistent LCAO-MO calculations on $(\text{GaN})_x$ and $(\text{GaN})_x\text{Cr}_2$ ($x \leq 3$) clusters, whose equilibrium geometries are shown in Fig. 4. We note that all the structures of $(\text{GaN})_x$ ($x \leq 3$) clusters are planar with strong Ga-N bonds. The GaN bond length in the dimer is 1.88 \AA , which is close to the Ga-N distance of 1.947 \AA in the bulk. The Ga-N bond distances increase somewhat with cluster size. These results

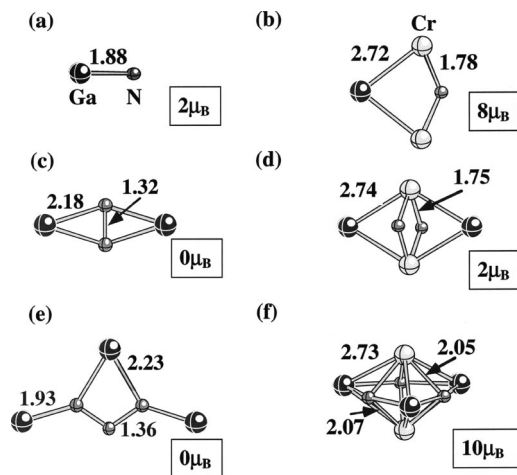


FIG. 4. Ground-state cluster geometries of $(\text{GaN})_x$ (left panel) and $(\text{GaN})_x\text{Cr}_2$ (right panel).

are in very good agreement with other available calculations.²⁴ This situation changes substantially when Cr atoms are added. The GaN bonds break in $(\text{GaN})_x$ ($x \leq 2$) clusters but reappear in $(\text{GaN})_3$, although in a stretched form. On the other hand, a Cr-N bond emerges and the corresponding bond length remains relatively unchanged throughout. The energy gains, Δ , in adding a Cr₂ dimer to an existing $(\text{GaN})_x$ cluster, namely, $\Delta = -[E(\text{GaN})_x\text{Cr}_2 - E(\text{GaN})_x - E(\text{Cr}_2)]$ are 5.43, 3.21, and 4.47 eV, respectively, for $x = 1, 2, 3$. The corresponding values of Cr-Cr distances are 3.29, 2.62, and 2.74 Å, respectively, for $x = 1, 2, 3$. In this context it is worth mentioning that the calculated binding energies of CrN and GaN are, respectively, 2.06 eV and 2.16 eV. Consequently it is energetically possible to replace Ga by Cr in GaN. Thus, the success of synthesizing Cr-doped GaN in single crystals may have a molecular origin.

We next discuss the magnetic configurations of these clusters. The total magnetic moments of $(\text{GaN})_x$ clusters are 2, 0, and $0\mu_B$, respectively, for $x = 1, 2, 3$, i.e., GaN clusters containing as few as two dimers cease to be magnetic. However, as Cr₂ is added, the magnetic nature changes completely. To determine the ground-state spin multiplicity ($M = 2S + 1$) of $(\text{GaN})_x\text{Cr}_2$ clusters, we had to optimize their geometries for each allowable M . In Fig. 5 we plot the energies of $\text{Cr}_2(\text{GaN})_x$ clusters as a function of M relative to the lowest energy configuration. The preferred spin multiplicity and hence, the total magnetic moment of these clusters correspond to the ground-state configuration. The total magnetic moment of $(\text{GaN})_1\text{Cr}_2$ is $8\mu_B$, out of which $0.07\mu_B$, $-0.64\mu_B$, and $4.28\mu_B$ moments are residing at Ga, N, and Cr sites, respectively. Note that the coupling between two Cr atoms is ferromagnetic while that between Cr and N is antiferromagnetic. It is well known²⁵ that in Cr₂, the spin coupling is antiferromagnetic when the Cr atoms are closer and it becomes ferromagnetic when the Cr-Cr distance increases. Therefore, we have calculated the antiferromagnetic state for $M = 1$ in the $(\text{GaN})_1\text{Cr}_2$ cluster. It does show a dip in total energy in Fig. 5. The spins at Ga and N are almost zero while those at the Cr sites are $+4.16\mu_B$ and $-4.16\mu_B$, respectively. However, as noted above, the ground state is ferromagnetic

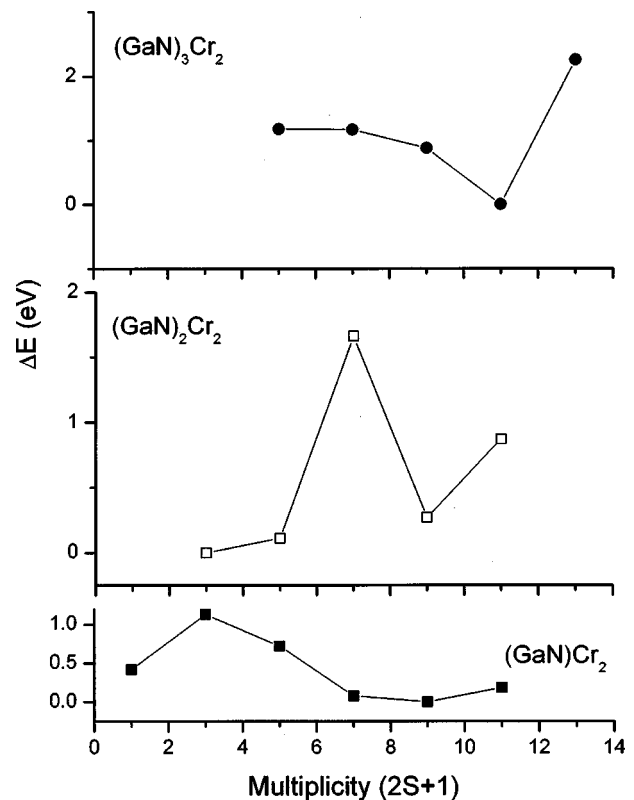


FIG. 5. Variation of total energy of $\text{Cr}_2(\text{GaN})_x$ ($x \leq 3$) clusters with spin multiplicity $(2S + 1)$. Energy ΔE (eV) is given with respect to the ground-state energy.

with a lowering of energy by 0.42 eV. In lower concentrations of Cr, the Cr-Cr distance will be even higher in the Cr-doped bulk GaN, and this should lead to ferromagnetic coupling between two Cr atoms. Therefore, we have not examined the $M = 1$ state for the other clusters. The results for spins at Ga, N, and Cr in $(\text{GaN})_2\text{Cr}_2$ and $(\text{GaN})_3\text{Cr}_2$ clusters follow the same pattern as that in $(\text{GaN})_1\text{Cr}_2$ although the magnitudes of the moments vary with size. In $(\text{GaN})_2\text{Cr}_2$, the moments at Ga, N, and Cr sites are, respectively, -0.32 , -0.32 , and $1.64\mu_B$. The total magnetic moment of $(\text{GaN})_2\text{Cr}_2$ is significantly reduced from that in $(\text{GaN})_1\text{Cr}_2$, namely, to $2\mu_B$ although Cr atoms remain ferromagnetically coupled. The total magnetic moment of $(\text{GaN})_3\text{Cr}_2$ rises sharply to $10\mu_B$, of which $0.66\mu_B$, $-0.04\mu_B$, and $4.07\mu_B$ moments reside at Ga, N, and Cr sites. Once again, the coupling between the Cr atoms is ferromagnetic and the critical separation needed is ~ 2.7 Å. In fact, for our supercell calculation we kept this Cr-Cr distance as 3.2 Å, as already mentioned in Sec. II A. It is important to note that the coupling between the Cr and the N atoms, which are strongly bonded to each other, remain antiferromagnetic irrespective of whether Cr is doped into clusters or crystal. This provides some insight into the origin of the ferromagnetic coupling between doped Cr atoms—namely, that it is an indirect exchange mechanism mediated by nitrogen.

IV. CONCLUSION

We have shown through first-principles calculations that the Cr atoms couple ferromagnetically when doped into GaN

whether the host is a cluster or a crystal. For Cr₂ in GaN, the ferromagnetic ground state is found to be 0.42 eV lower than the antiferromagnetic one. This coupling is mediated by nitrogen through an indirect exchange mechanism and is a local phenomenon (also see the conclusions of Ref. 10). The magnetic moment per Cr atom is about $4\mu_B$ in clusters, while it is about $2.69\mu_B$ in bulk GaN crystal. That the coupling is ferromagnetic irrespective of the host structure allows great

flexibility in synthesizing DMS systems involving Cr-doped GaN.

ACKNOWLEDGMENT

This work was supported in part by a grant from the Department of Energy (Grant No. DEFG02-96ER45579).

-
- ¹H. Ohno, *Science* **281**, 951 (1998).
²T. Dietl, H. Ohno, F. Matsukura, J. Cibert, and D. Ferrand, *Science* **287**, 1019 (2000).
³T. Dietl, *Semicond. Sci. Technol.* **17**, 377 (2002), and references therein.
⁴H. Morkoc, *Nitride Semiconductors and Devices* (Springer-Verlag, Berlin, 1999), enlarged second edition to be published in 2002.
⁵S. E. Park, H. -J. Lee, Y. C. Cho, S.-Y. Jeong, C. R. Cho, and S. Cho, *Appl. Phys. Lett.* **80**, 4187 (2002).
⁶M. L. Reed, N. A. El-Masry, H. H. Stadelmaier, M. K. Ritums, M. J. Reed, C. A. Parker, and S. M. Bedair, *Appl. Phys. Lett.* **79**, 3473 (2001).
⁷M. Hashimoto, Y.-K. Zhou, M. Kanamura, and H. Asahi, *Solid State Commun.* **122**, 37 (2002).
⁸C. Zener, *Phys. Rev.* **82**, 403 (1951).
⁹V. I. Litinov and V. K. Dugaev, *Phys. Rev. Lett.* **86**, 5593 (2001).
¹⁰M. van Schilfgaarde and O. N. Mryasov, *Phys. Rev. B* **63**, 233205 (2001).
¹¹L. Kronik, M. Jain, and J. R. Chelikowsky, *Phys. Rev. B* **66**, 041203(R) (2002).
¹²K. Sato and H. Katayama-Yoshida, *Semicond. Sci. Technol.* **17**, 367 (2002); K. Sato *et al.*, *Jpn. J. Appl. Phys., Part 2* **40**, L485 (2001).
¹³B. K. Rao and P. Jena, *Phys. Rev. Lett.* **89**, 185504 (2002).
¹⁴J. P. Perdew and Y. Wang, *Phys. Rev. B* **33**, 8800 (1986); J. P. Perdew, *ibid.* **33**, 8822 (1986); J. P. Perdew and Y. Wang, *ibid.* **45**, 13244 (1992).
¹⁵O. K. Andersen and O. Jepsen, *Phys. Rev. Lett.* **53**, 2571 (1984); O. K. Andersen, *Phys. Rev. B* **12**, 3060 (1975). We have used the latest version of the Stuttgart TB-LMTO-ASA program.
¹⁶N. E. Christensen and I. Gorczyca, *Phys. Rev. B* **50**, 4397 (1994).
¹⁷C. G. van de Walle, S. Limpijumngong, and J. Neugebauer, *Phys. Rev. B* **63**, 245205 (2001).
¹⁸O. Jepsen and O. K. Andersen, *Z. Phys. B: Condens. Matter* **97**, 35 (1995).
¹⁹P. Bloechl, O. Jepsen, and O. K. Andersen, *Phys. Rev. B* **49**, 16223 (1994).
²⁰GAUSSIAN 98, Revision A.7, M. J. Frisch *et al.*, Gaussian, Inc., Pittsburgh, PA, 1998.
²¹A. D. Becke, *Phys. Rev. A* **38**, 3098 (1988); J. P. Perdew, K. Burke, and Y. Wang, *Phys. Rev. B* **54**, 16533 (1996); K. Burke, J. P. Perdew, and Y. Wang, in *Electronic Density Functional Theory: Recent Progress and New Directions*, edited by J. F. Dobson, G. Vignale, and M. P. Das (Plenum, New York, 1998).
²²Just as density of states are projected onto different sites and orbitals, energy bands can also be projected onto different site orbitals. Some of these can be “fattened” in order to distinguish them from the rest of the band structure. These projected fattened bands are called the “fat bands.” For more details, see O. Jepsen and O. K. Andersen, *Z. Phys. B: Condens. Matter* **97**, 35 (1995).
²³G. P. Das, B. K. Rao, and P. Jena, *Phys. Rev. B* **68**, 035207 (2003).
²⁴A. K. Kandalam, R. Pandey, M. A. Blanco, A. Costales, J. M. Recio, and J. M. Newsam, *J. Phys. Chem. B* **104**, 4361 (2001); A. K. Kandalam, M. A. Blanco, and R. Pandey, *ibid.* **105**, 6080 (2001).
²⁵N. Desmarais, F. A. Reuse, and S. N. Khanna, *J. Chem. Phys.* **112**, 5576 (2000).